

# Rigorous study of short periodic orbits for the Lorenz system

Zbigniew Galias

Department of Electrical Engineering

AGH — University of Science and Technology  
al. Mickiewicza 30, 30–059 Kraków, Poland  
Email: galias@agh.edu.pl

Warwick Tucker

Department of Mathematics

University of Bergen  
Johannes Bruns gate 12, 5008 Bergen, Norway  
Email: warwick.tucker@math.uib.no

**Abstract**—The existence of short periodic orbits for the Lorenz system is studied rigorously. We describe a method for finding all short cycles embedded in a chaotic singular attractor (i.e. an attractor containing an equilibrium). The method uses an interval operator for proving the existence of periodic orbits in regions where it can be evaluated, and bounds for the return time in other regions. The six shortest periodic orbits for the Lorenz system are found.

## I. INTRODUCTION

Proving the existence of periodic orbits for nonlinear continuous-time systems is usually not a trivial task. An important class of methods use interval operators applied to a Poincaré map associated with the continuous system considered. When these methods are combined with the method of close returns, which provides initial guesses for positions of periodic orbits, they can be used to extract many cycles embedded in chaotic attractors.

Finding all short periodic orbits is even more difficult. It is known that this problem can be successfully solved for a certain class of systems including the Rössler system [1]. In this work we extend this method to a class of systems, whose attractors (like the Lorenz attractor) contain an unstable equilibrium. For such systems there exist trajectories for which the return time is arbitrarily long. It is impossible to evaluate an interval operator over a box containing such trajectories. For nearby boxes the evaluation procedure often fails or produces unusable results due to huge overestimation.

The Lorenz system [2] is well understood in terms of geometric models [3]. It has been shown to be chaotic in the topological sense for the case of non-classical [4] and classical [5] parameter values. The existence of the Lorenz attractor has been shown in [6]. In this work, we present first results on the existence of short periodic orbits for the Lorenz system. To our knowledge this has not been done before. We find the six shortest periodic orbits for the Lorenz system, and show that there are no shorter periodic orbits.

## II. INTERVAL METHODS FOR FINDING ALL SHORT CYCLES

In this section, we briefly describe a general method which can be used to find all short periodic orbits. The first step of the method is a reduction of the continuous-time system to a discrete system using the concept of the Poincaré map.

### A. Poincaré map

Let us choose hyperplanes  $\Sigma_1, \Sigma_2, \dots, \Sigma_m$  and let  $\Sigma = \Sigma_1 \cup \dots \cup \Sigma_m$ . The Poincaré map  $P : \Sigma \mapsto \Sigma$  is defined as

$$P(x) = \varphi(\tau(x), x), \quad (1)$$

where  $\tau(x)$  is the return time after which the trajectory  $\varphi(t, x)$  returns to  $\Sigma$ . Periodic points of  $P$  correspond to periodic orbits of the continuous system.

In order to study the existence of period- $n$  orbits of  $P$  we construct the map  $F$  defined by

$$[F(z)]_k = x_{(k \bmod n)+1} - P(x_k), \quad k = 1, \dots, n, \quad (2)$$

where  $z = (x_1, \dots, x_n)^T$ . Zeros of  $F$  correspond to period- $n$  orbits of  $P$ , i.e.  $F(z) = 0$  if and only if  $P^n(x_1) = x_1$ .

### B. Interval methods

Interval methods provide simple computational tests for uniqueness, existence, and nonexistence of zeros of a map within a given interval vector. In order to investigate the existence of zeros of  $F$  in the interval vector  $\mathbf{z}$  one evaluates an interval operator over  $\mathbf{z}$ . In this work we use the Krawczyk operator [7]. There are other possible choices, like the interval Newton operator or Hansen–Sengupta operator, but in this case they are outperformed by the Krawczyk method. The *Krawczyk operator* is defined as

$$K(\mathbf{z}) = \hat{\mathbf{z}} - CF(\hat{\mathbf{z}}) - (CF'(\mathbf{z}) - I)(\mathbf{z} - \hat{\mathbf{z}}), \quad (3)$$

where  $\hat{\mathbf{z}} \in \mathbf{z}$  and  $C$  is an invertible matrix. In our implementation, we choose  $\hat{\mathbf{z}}$  to be the center of  $\mathbf{z}$ , and the preconditioning matrix  $C$  to be the inverse of  $F'(\hat{\mathbf{z}})$ .

If  $K(\mathbf{z})$  is enclosed in the interior of  $\mathbf{z}$ , i.e.  $K(\mathbf{z}) \subset \text{int } \mathbf{z}$ , then  $F$  has exactly one zero in  $\mathbf{z}$ . This property allows us to prove the existence and uniqueness of zeros. If  $K(\mathbf{z}) \cap \mathbf{z} = \emptyset$ , then there are no zeros of  $F$  in  $\mathbf{z}$ .

In order to evaluate the interval operator for the map  $F$  defined by Eq. (2), we need a method to find an enclosure of  $P(\mathbf{x})$  and an enclosure of the Jacobian  $P'(\mathbf{x})$ . These enclosures are found in interval arithmetic by rigorous integration of the differential equation and its variational equation. For details see [1].

### C. Finding all short cycles

The method to find all periodic orbits of  $P$  belonging to a certain region starts with covering the region of interest by boxes — interval vectors. Next, dynamics of  $P$  is represented in the form of a directed graph, where boxes are the vertices of the graph and non-forbidden connections are graph edges. This representation is found rigorously by computing for each box  $\mathbf{v}_i$  an enclosure  $\mathbf{w}_i$  of its image  $P(\mathbf{v}_i)$ , and finding all boxes which have nonempty intersection with  $\mathbf{w}_i$ .

In the second step all period- $n$  cycles in the graph are found. Finally, for each cycle the interval operator is evaluated over the corresponding interval vector  $\mathbf{z}$ . If  $\mathbf{z} \cap K(\mathbf{z}) = \emptyset$ , then there are no period- $n$  orbits in  $\mathbf{z}$ . If  $K(\mathbf{z}) \subset \text{int } \mathbf{z}$ , then there exists exactly one period- $n$  orbit inside  $\mathbf{z}$  ( $n$  is possibly not the basic period of the orbit). If neither of the above two conditions is satisfied the search procedure fails, and we may try to repeat the computation using smaller boxes.

## III. SHORT PERIODIC ORBITS FOR THE LORENZ SYSTEM

### A. Lorenz system

The Lorenz system is described by the following set of equations

$$\begin{aligned}\dot{x}_1 &= sx_2 - sx_1, \\ \dot{x}_2 &= rx_1 - x_2 - x_1x_3, \\ \dot{x}_3 &= x_1x_2 - qx_3.\end{aligned}\tag{4}$$

We consider the Lorenz system with the classical parameter values:  $s = 10$ ,  $r = 28$ ,  $q = 8/3$ .

In the following we use the diagonal form of the Lorenz system (it can be obtained using a linear change of variables), where the invariant manifolds of the origin are tangent to the coordinate axes:

$$\begin{aligned}\dot{x}_1 &= \lambda_1 x_1 - k_1(x_1 + x_2)x_3, \\ \dot{x}_2 &= \lambda_2 x_2 + k_1(x_1 + x_2)x_3, \\ \dot{x}_3 &= \lambda_3 x_3 + (x_1 + x_2)(k_2 x_1 + k_3 x_2).\end{aligned}\tag{5}$$

The constants are given by

$$\begin{aligned}u &= \sqrt{(s+1)^2 + 4s(r-1)}, \\ k_1 &= s/u \approx 0.2886, \quad k_2 = (s-1+u)/(2s) \approx 2.1828, \\ k_3 &= (s-1-u)/(2s) \approx -1.2828, \\ \lambda_1 &= (-s-1+u)/2 \approx 11.8277, \\ \lambda_2 &= (-s-1-u)/2 \approx -22.8277, \\ \lambda_3 &= -q \approx -2.6667.\end{aligned}\tag{6}$$

From now on we will refer to (5) as the Lorenz system. A trajectory of the Lorenz system is shown in Fig. 1.

For the parameter values we consider, the Lorenz system has three equilibria. One of them is the origin  $P_0 = (0, 0, 0)^T$ . It has one positive eigenvalue  $\lambda_1$  and two negative eigenvalues  $\lambda_2$  and  $\lambda_3$  defined in (6). The coordinates of the other two equilibria, shown in Fig. 1 using symbols  $\times$  and  $+$ , are

$$P_{\pm} = \left( \mp \frac{\lambda_2}{u} \sqrt{q(r-1)}, \pm \frac{\lambda_1}{u} \sqrt{q(r-1)}, r-1 \right).$$

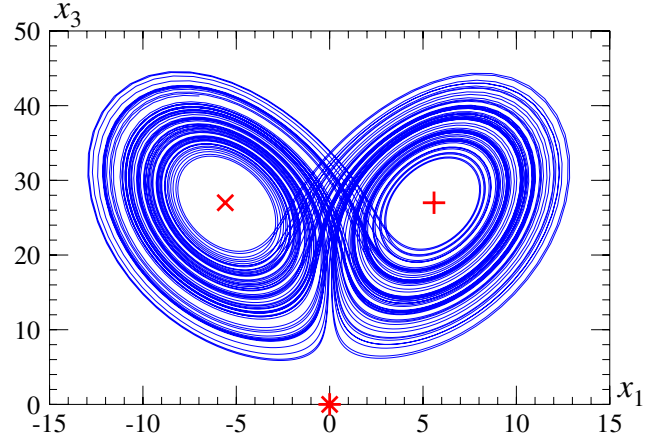


Fig. 1. A trajectory of the Lorenz system

$P_{\pm} \approx (\pm 5.589, \pm 2.896, 27)$  have a pair of complex eigenvalues with positive real parts  $\mu_{1,2} \approx 0.094 \pm j10.19$ , and one real negative eigenvalue  $\mu_3 \approx -13.854$ .

### B. Trapping region and average return time

Let us choose the Poincaré map  $P$  defined by the section  $\Sigma = \{x = (x_1, x_2, x_3) : x_3 = r-1, \dot{x}_3 < 0\}$ .

We begin our analysis of the existence of periodic orbits in the Lorenz attractor by finding a trapping region containing the attractor of  $P$ . Observe that this cannot be done by a direct integration of the differential equation seeing that there are trajectories in the Lorenz attractor which pass arbitrarily close to the origin, and for which the return time is arbitrarily long. The trapping region is found using a modified Euler method with rigorous error bounds. In order to reduce expansion along the trajectories we use partitioning. When a box has expanded enough, it is partitioned, and the sub-boxes are then treated separately. This helps reduce the problems associated with the wrapping effect. Trajectories passing close to the fixed point at the origin are treated differently. We define a cube around the origin, and interrupt computations if the trajectory hits the cube. We then change to the normal form coordinates and explicitly compute the exit of the trajectory. There are two different ways in which a rectangle can pass through the cube. If the box intersects the stable manifold of the origin, it is split along the line of intersection, and exits the cube in two pieces. Otherwise, the box flows out in one piece. After leaving the cube, we switch back to the original coordinates, and resume numeric computations. For details see [6].

The trapping region is composed of 14518 boxes of size  $1/2^7 \times 1/2^7$  (see Fig. 2). There are 514126 connections in the corresponding graph.

Using information on return times for individual boxes, we can find bounds for the return time for the  $n$ th iterate of  $P$ . Since for some boxes an upper bound for the return time is infinite, the return time for the whole attractor is unbounded. Lower bounds of return times are collected in Table I.

It is clear that the average return time  $\tau_{\text{aver}}$  between two

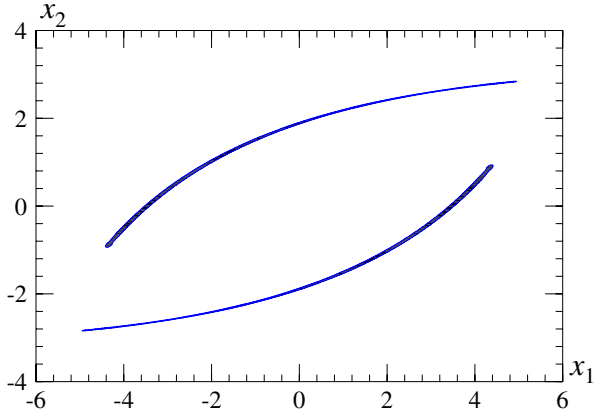


Fig. 2. Trapping region for the Poincaré map,  $x_3 = 27$

TABLE I  
LOWER BOUND  $t_n$  OF RETURN TIMES FOR  $P^n$

$n$	$t_n$	$t_n/n$
1	0.537044	0.537044
2	1.147434	0.573717
5	2.981325	0.596265
10	6.047894	0.6047894
100	63.721019	0.63721019
10000	6397.362682	0.6397362682

crossings is larger than  $t_n/n$  for each  $n$ . For  $n = 10000$  we obtain:

$$\tau_{\text{aver}} > 0.6397. \quad (7)$$

It follows that the length of any periodic orbit corresponding to a period- $n$  cycle of  $P$  is larger than  $n \cdot 0.6397$ .

### C. Periodic orbits

There are no period-1 cycles in the graph, hence there are no period-1 orbits.

In order to study the existence of period-2 orbits, a set of boxes containing all period-2 cycles is found. This set is composed of 86 boxes, and is shown in Fig. 3(a).

The application of the method for finding all period-2 orbits is unsuccessful for this set due to long return times and too strong stretching. We have to introduce more sections for the Poincaré map to make the return time shorter. Let us now consider the Poincaré map  $P_1$  corresponding to  $\Sigma = \Sigma_1 \cup \Sigma_2$ , where  $\Sigma_1 = \{x: x_3 = 27\}$ ,  $\Sigma_2 = \{x: x_3 = 14\}$ . Clearly, period-2 orbits of the original map  $P$  correspond to period-8 orbits of the map  $P_1$ . We start by generating the graph for  $P_1$ . The graph has 182 boxes and 638 connections. There are 26086 period-8 cycles in the graph. In order to reduce the number of cycles, we regenerate the graph at higher accuracy, and then come back to the original box size. This procedure significantly reduces the number of cycles to be considered.

Dividing each box into  $16 \times 16$  smaller boxes, and generating the graph for this division we arrive at a covering composed of 216 boxes of size  $1/2^{11} \times 1/2^{11}$  with 724 connections. Coming back to the original box size gives 16 boxes and 24 connections.

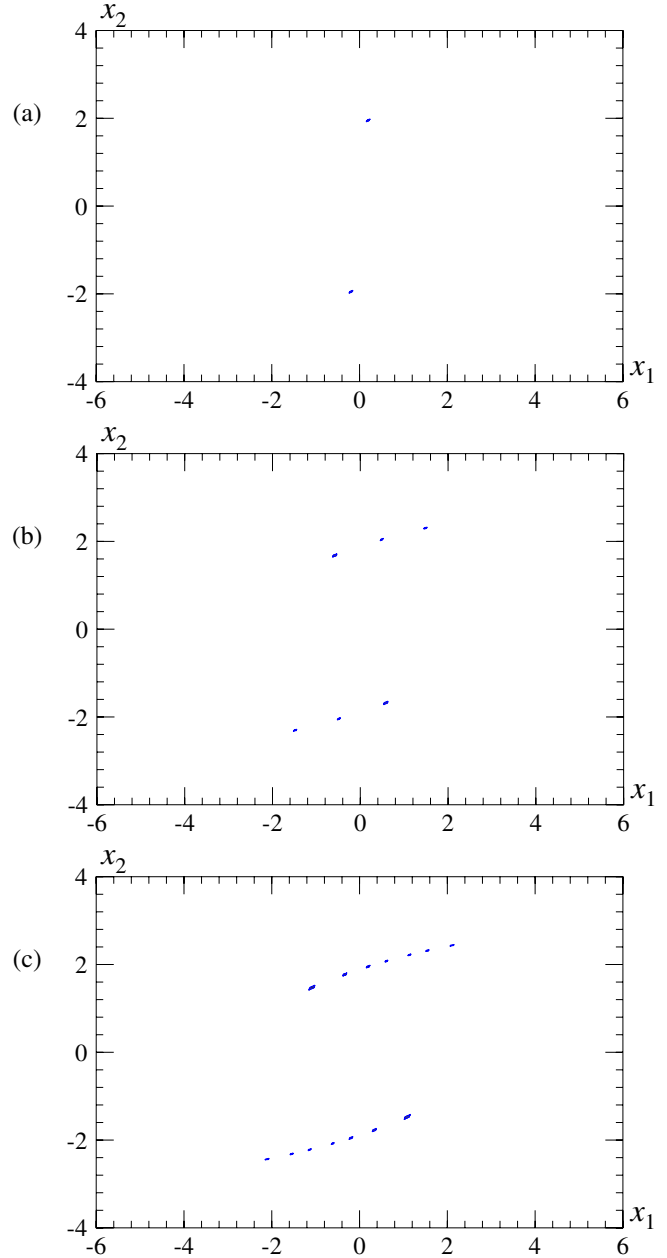


Fig. 3. Regions containing all periodic orbits with period  $p=2,3,4$ ,  $x_3 = 27$

At this stage we can apply the techniques described in Section II to find all period-2 orbits of  $P$ . There are 36 cycles of length 8. The Krawczyk operator is evaluated for each cycle, and it is verified that only one of them corresponds to a periodic orbit. It is shown in Fig. 4(a). Note that this periodic orbit is self-symmetric.

Similar computations have been performed for period  $p = 3, 4$ . The set containing all period-3 cycles is composed of 254 boxes (see Fig. 4(b)). Introducing sections  $\Sigma_1 = \{x: x_3 = 27\}$ ,  $\Sigma_2 = \{x: x_3 = 18\}$  we obtain a graph composed of 636 cycles and 2748 connections. To reduce the number of cycles, we consider boxes of size  $1/2^{13} \times 1/2^{13}$ . The resulting graph

TABLE II  
SHORT PERIODIC ORBITS, PERIOD  $p$  OF THE ASSOCIATED PERIODIC ORBIT  
OF  $P$ , AND LENGTH  $t$

	$p$	$t$
1	2	[1.55802, 1.55929]
2	3	[2.30589, 2.30592]
3	3	[2.30589, 2.30592]
4	4	[3.02335, 3.02382]
5	4	[3.02335, 3.02382]
6	4	[3.08426, 3.08429]

has 460 boxes and 1500 connections. Increasing the box size, we obtain a set of 38 boxes of size  $1/2^9 \times 1/2^9$  with 54 connections. There are 72 period-12 cycles in the graph. Two of them correspond to periodic orbits. They are symmetric to each other. One of them is shown in Fig. 4(b).

For the case  $p = 4$  there are 654 boxes covering period-4 orbits of  $P$ . Using sections  $\Sigma_1 = \{x: x_3 = 27\}$ ,  $\Sigma_2 = \{x: x_3 = 19\}$  we obtain a graph composed of 2220 boxes with 15516 connections. Considering the box size  $1/2^{17} \times 1/2^{17}$ , we obtain 3166 boxes with 21450 connections. Increasing the box size, we obtain a set of 72 boxes of size  $1/2^{10} \times 1/2^{10}$  with 90 connections. Out of 188 period-16 cycles three correspond to periodic orbits. There is a pair of orbits symmetric to each other (one of them is shown in Fig. 4(c)) and a self-symmetric orbit (Fig. 4(d)).

Lengths of the periodic orbits found are reported in Table II.

Since all periodic orbits of period  $p \leq 4$  have been found, the length of each orbit found is shorter than 3.1, and the length of any other periodic orbit is larger than  $5 \cdot 0.6397 = 3.1985$  (compare Eq. (7)), it follows that the periodic orbits found are shortest.

#### IV. CONCLUSION

We have described a method which can be used for finding all periodic orbits up to a certain length for continuous-time systems with Poincaré maps having unbounded return times. The method has been applied to the Lorenz system for which the six shortest periodic orbits have been located.

#### ACKNOWLEDGMENT

This work was supported in part by the AGH University of Science and Technology, grant no. 10.10.120.133.

#### REFERENCES

- [1] Z. Galias, "Counting low-period cycles for flows," *Int. J. Bifurcation and Chaos*, vol. 16, no. 10, pp. 2873–2886, 2006.
- [2] E. Lorenz, "Deterministic non-periodic flow," *Journal of Atmospheric Science*, vol. 20, pp. 130–141, 1963.
- [3] C. Sparrow, *The Lorenz equations: Bifurcations, Chaos, and Strange Attractors*. New York: Springer Verlag, 1982.
- [4] K. Mischaikow and M. Mrozek, "Chaos in the Lorenz equations: a computer assisted proof," *Bull. Amer. Math. Soc.*, vol. 32, no. 1, pp. 66–72, 1995.
- [5] Z. Galias and P. Zgliczyński, "Computer assisted proof of chaos in the Lorenz equations," *Physica D*, vol. 115, pp. 165–188, 1998.
- [6] W. Tucker, "The Lorenz attractor exists," *C. R. Acad. Sci. Paris*, vol. 328, pp. 1197–1202, 1999.
- [7] A. Neumaier, *Interval methods for systems of equations*. Cambridge University Press, 1990.

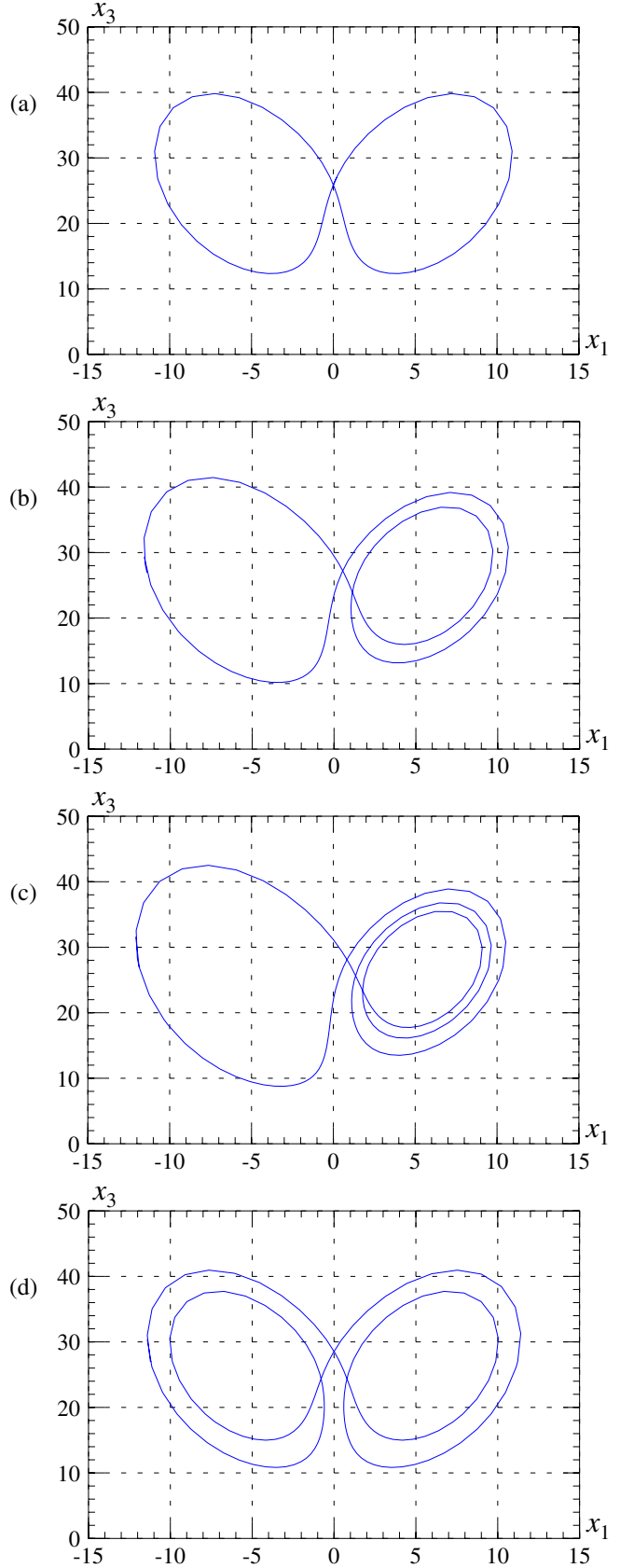


Fig. 4. Short periodic orbits